Carbohydrate Polymers 98 (2013) 233–240

Contents lists available at SciVerse ScienceDirect

Carbohydrate Polymers

journal homepage: www.elsevier.com/locate/carbpol

Development of cesium phosphotungstate salt and chitosan composite membrane for direct methanol fuel cells

Yanxin Xiao[a,b,1], Yan Xiang[a,b,1], Ruijie Xiu[a,b], Shanfu Lu[a,b,*]

[a] Key Laboratory of Bio-Inspired Smart Interfacial Science and Technology of Ministry of Education, School of Chemistry and Environment, Beihang University, Beijing, 100191, PR China

[b] Beijing Key Laboratory of Bio-Inspired Energy Materials and Devices, School of Chemistry and Environment, Beihang University, Beijing, 100191, PR China

ARTICLE INFO

Article history:
Received 2 May 2013
Received in revised form 10 June 2013
Accepted 15 June 2013
Available online 20 June 2013

Keywords:
Cesium phosphotungstate salt
Chitosan
Alternative proton exchange membranes
Methanol crossover
Direct methanol fuel cells

ABSTRACT

A novel composite membrane has been developed by doping cesium phosphotungstate salt ($Cs_xH_{3-x}PW_{12}O_{40}$ ($0 \le x \le 3$), Cs_x-PTA) into chitosan (CTS/Cs_x-PTA) for application in direct methanol fuel cells (DMFCs). Uniform distribution of Cs_x-PTA nanoparticles has been achieved in the chitosan matrix. The proton conductivity of the composite membrane is significantly affected by the Cs_x-PTA content in the composite membrane as well as the Cs substitution in PTA. The highest proton conductivity for the CTS/Cs_x-PTA membranes was obtained with $x = 2$ and Cs_2-PTA content of 5 wt%. The value is 6×10^{-3} S cm^{-1} and 1.75×10^{-2} S cm^{-1} at 298 K and 353 K, respectively. The methanol permeability of CTS/Cs_2-PTA membrane is about 5.6×10^{-7}, 90% lower than that of Nafion-212 membrane. The highest selectivity factor (φ) was obtained on CTS/Cs_2-PTA-5 wt% composite membrane, 1.1×10^4/S cm^{-3} s. The present study indicates the promising potential of CTS/Cs_x-PTA composite membrane as alternative proton exchange membranes in direct methanol fuel cells.

1. Introduction

Direct methanol fuel cells (DMFCs) have been considered as attractive alternative energy supply for future portable electronic devices due to their capability of high energy density, simplified system design and convenient fuel transportation and storage (Jiang, Zheng, Wu, Wang, & Wang, 2008; Tang, Wang, Pan, Jiang, & Ruan, 2007). The most common proton exchange membranes used in DMFCs are the state-of-the-art perfluorosulfonic acid (PFSA) based membranes such as Nafion due to their high proton conductivity, high structural and chemical stability and mechanical strength (Chai et al., 2010; Tang, Pan, & Wang, 2008). However, PFSA based membranes such as Nafion exhibit two technical challenges. One is their high cost (Sancho, Soler, & Pina, 2007), and the other is methanol crossover from anode to cathode through the membrane which results in a significant reduction in the electrical performance of DMFCs (Du, Zhao, & Yang, 2007; Eccarius, Garcia, Hebling, & Weidner, 2008; Qi & Kaufman, 2002; Tang, Pan, Jiang, & Yuan, 2005; Yang & Bae, 2008). It has been reported that over 40% of methanol could be lost in a DMFC due to crossover across the membrane (Tricoli, Carretta, & Bartolozzi, 2000).

In the past several years, much effort has been made in the development of polymer electrolyte membrane with inherent low methanol permeability, high conductivity and lower cost. Among them, chitosan (CTS) based materials have shown promising properties for applications as proton exchange membranes of low temperature fuel cells (Ma & Sahai, 2013; Odeh, Osifo, & Noemagus, 2013). Chitosan is an abundant natural polymer with low toxicity, biodegradable and biocompatible properties (Muzzarelli, 2011) that has been intensely used as a promising and low cost source of membrane material (Cui et al., 2008; Ma, Sahai, & Buchheit, 2012; Osifo & Masala, 2012). The wide application of chitosan on pervaporation membrane revealed its fine methanol permeability (Ghazali, Nawawi, & Huang, 1997; Mochizuki, Amiya, Sato, Ogawara, & Yamashita, 1989). Furthermore, chitosan based materials exhibit good thermal/chemical stability and mechanical properties due to the ring structure of the

Abbreviations: CTS, chitosan; PTA, phosphotungstate salt; Cs_xPTA, cesium phosphotungstate salt ($0 \le x \le 3$); CTS/Cs_xPTA, cesium phosphotungstate salt and chitosan composite membrane; φ, selectivity factor; HPAs, heteropolyacids; WU, water uptake; W_{wet}, weight of wet membrane; W_{dry}, weight of dry membrane; ΔS, swelling degree; S_{wet}, area of wet membrane; S_{dry}, area of the dry membrane; σ, proton conductivity; GC, gas chromatography; FID, hydrogen flame ionization; P, methanol diffusion coefficient; NPs, nanoparticles.

* Corresponding author at: Key Laboratory of Bio-Inspired Smart Interfacial Science and Technology of Ministry of Education, School of Chemistry and Environment, Beihang University, Beijing, 100191, PR China. Tel.: +86 10 82339539; fax: +86 10 82339539.
E-mail address: lusf@buaa.edu.cn (S. Lu).

[1] Both authors contributed equally to this work.

0144-8617/$ – see front matter © 2013 Elsevier Ltd. All rights reserved.
http://dx.doi.org/10.1016/j.carbpol.2013.06.017

chitosan molecular, which would be beneficial to the fuel cell operation. However, pristine chitosan has low conductivity and there are no mobile hydrogen ions in its structure. It has been reported that the proton conductivity of the dry chitosan film without cross-linking and modification is very low, $\sim 10^{-9}$ S cm^{-1} at room temperature (Suzuki, Saimoto, & Shigemasa, 1999; Wan, Creber, Peppley, & Bui, 2003a). In order to increase the ionic conductivity of CTS membranes, structural modification (Chávez, Oviedo-Roa, Contreras-Pérez, Martínez-Magadán, & Castillo-Alvarado, 2010; Wan, Creber, Peppley, & Bui, 2003b), blending (Seo, Koh, Roh, & Kim, 2009; Smitha, Sridhar, & Khan, 2005), proton acid doping (Cui, Xing, Liu, Liao, & Zhang, 2009; Ma et al., 2012; Smitha, Devi, & Sridhar, 2008; Yamada & Honma, 2005) and inorganic salts doping (Khiar, Puteh, & Arof, 2006; Majid & Arof, 2005; Wu, Hou, Wang, Xiao, & Jiang, 2010) methods have been introduced. These studies have showed that the proton conductivity of the chitosan membrane could be improved while maintaining its good mechanical properties, methanol permeability and thermal/chemical stability.

Heteropolyacids (HPAs) are well known as superionic conductors in their fully hydrated state, particularly those with Keggin structure (Yang et al., 2005) and have been used to enhance the proton conductivity, water retention and resistance to methanol crossover properties of Nafion or other proton exchange membranes (Li, Xu, & Wang, 2003; Yang, Lu, Lu, Jiang, & Xiang, 2010). Among HPAs, cesium phosphotungstate salt (Cs_x-PTA, $0 \leq x \leq 3$) which contains the characteristic structure of phosphotungstic acid (PTA), has excellent conductive capability and increased stability in aqueous medium (Matsuda et al., 2007). It has been shown that addition of Cs_x-PTA enhances the proton conductivity and reduced methanol permeability of host matrix materials including sulfonated poly (ether-ether ketone) (SPEEK) (Doğan, Inan, Unveren, & Kaya, 2010; Zhang, Zhang, & Bi, 2008), Nafion (Amirinejad, Madaeni, & Navarra, 2011; Amirinejad, Madaeni, & Rafiee, 2011), chitosan-hydroxy ethyl cellulose (CS-HEC) (Mohanapriya et al., 2009), polybenzimidazole (PBI) (Li, Shao, & Scott, 2008; Oh et al., 2010), Nafion/polytetrafluoroethylene (PTFE) (Li, Shao, & Zhang, 2006) and polyethyleneoxide (PEO)/polyvinylidene fluoride–chlorotetrafluoroethylene (PVDF–CTFE) copolymer (Amirinejad, Madaeni, Navarra, Rafiee, & Scrosati, 2010), etc. As indicated by Hacer Dogan (Doğan et al., 2010), the methanol permeability was reduced to 4.7×10^{-7} cm^2/s for SPEEK/Cs-PTA membrane with 10 wt% Cs-PTA concentration, and acceptable proton conductivity of 1.3×10^{-1} S/cm was achieved at 80 °C under 100% RH.

In the present study, CTS/Cs_x-PTA composite membrane was prepared by blending Cs_x-PTA ($0 \leq x \leq 3$) with chitosan/acetic acid solution for potential application as proton exchange membranes of DMFCs. The composite membranes were characterized in details by Fourier transform infrared (FT-IR), X-ray diffraction (XRD), scanning electron microscopy (SEM), energy dispersive X-ray (EDS) and thermo-gravimetric analysis (TG). Moreover, the effects of Cs_x-PTA content on the mechanical property and the proton conductivity at different temperatures, as well as the selectivity factor of CTS/Cs_x-PTA composite membrane has been investigated.

2. Experimental

2.1. Preparation of Cs_x-PTA and composite membranes

$Cs_xH_{3-x}PW_{12}O_{40}$ ($0 \leq x \leq 3$) were synthesized according to the literature method (Ma, Hua, Ren, He, & Gao, 2003). In a typical synthesis process, an aqueous solution of Cs_2CO_3 (0.1 mol/l) was added drop wise to an aqueous solution of $H_3PW_{12}O_{40}$ (PTA, Aldrich) (0.08 mol/l) with Cs/P molar ratios of 0.5, 1.0, 1.5, 2.0, 2.5, and 3.0, respectively, at room temperature under vigorous stirring. The resulting white colloidal solution was aged overnight at ambient temperature and then evaporated at 50 °C till it was dry. The obtained samples were denoted as Cs_x-PTA.

The Cs_2-PTA powders with 1, 5 and 10 wt% proportions were added to a 2% (w/v) chitosan–acetic acid solution. After complete dispersion, the solution was cast on a glass plate and dried at 333 K for 24 h. The dry membranes on the plates were striped from the plate and then immersed in the absolute methanol (Sigma–Aldrich) for 2 h to remove the acetic acid. Finally, the prepared membranes were used for analysis without further treatment. CTS with 1, 5 and 10 wt% Cs_2-PTA was denoted as CTS/Cs_2-PTA-1 wt%, CTS/Cs_2-PTA-5 wt%, CTS/Cs_2-PTA-10 wt%, respectively.

2.2. Characterization of CTS/Cs_2-PTA membranes

Both the surface and cross section morphology of CTS/Cs_2-PTA membranes were examined under a scanning electron microscope equipped with energy dispersive X-ray spectrometer (EDS) detector (SEM, Oxford, Camscan3400; Oxford Instruments). Elemental mapping analysis was used to study the distribution of typical elements tungsten (W) of PTA in the structure of composite membrane.

Fourier transform infrared (FT-IR) spectroscopy of the membranes was recorded with a Nicolet (Madison, WI, USA) AVATAR 470 Fourier transform infrared spectrometer in the wavelength range from 4000 to 500 cm^{-1}. X-ray diffraction (XRD) patterns for polymeric membrane and Cs_x-PTA powder were obtained on a D/max 2200PC X-ray diffract meter using Cu Kα radiation source operating at 40 kV and 30 mA. The scanning rate was 4°/min in the angular range of 5–60°.

Thermal stability of the polymer electrolyte membranes was tested by TG analysis. Membrane samples for TG analysis were cut to small pieces before the test. Then the samples were encapsulated in hermetically sealed aluminum pans. The thermal analysis was performed by Shimadzu TGA-50 thermal analysis system with heating rate of 10 °C/min under N_2 atmosphere.

To investigate the swelling behaviors of the composite electrolyte membrane, the membrane samples were cut and stored in a hydration-controlled container. To determine the water uptake (WU) at each state of hydration, the membranes were removed from the container using a filter paper to remove excess surface water, and quickly weighed to give the initial wet weight, $M_{wet.}$ The dry weight of the membrane samples, M_{dry} was obtained after drying at oven. Meanwhile, the areas, S of wet and dry samples was measured. The changes in water uptake and areas were calculated with the following equations (Tang, Wang, Pan, & Wang, 2007).

$$\text{Wateruptake}\,(\%) = \frac{M_{wet} - M_{dry}}{M_{dry}} \times 100 \quad (1)$$

$$\Delta S\,(\%) = \frac{S_{wet} - S_{dry}}{S_{dry}} \times 100 \quad (2)$$

where S_{wet} is the area of wet membrane sample, and S_{dry} is the area of the dry membrane sample.

The tensile strength and elongation of the composite membranes were evaluated by a tensile test instrument (INSTRON 3365). The test was carried out at a strain rate of 5 mm/min at 293 K and a relative humidity of ~10%. The membrane samples were prepared in rectangular shape with a gauge length of 40 mm and a width of 8 mm. The data of tensile strength elongation were determined according to the stress–strain curve. Each data was the average of at least three parallel experiments.

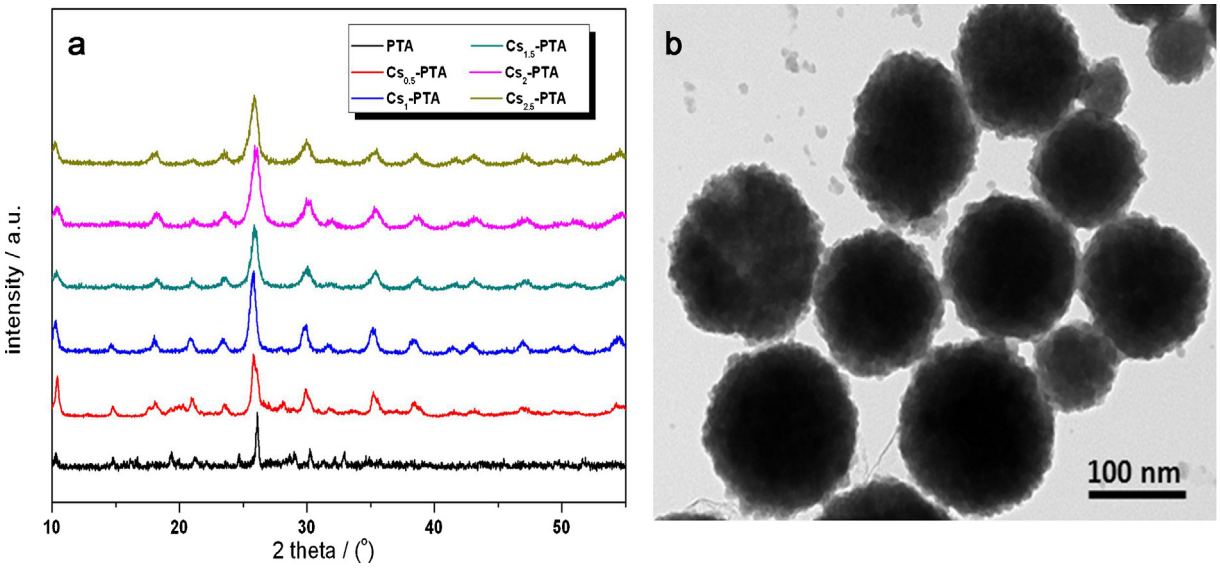

Fig. 1. (a) X-ray diffraction patterns of Cs_x-PTA with different x value (x = 0, 0.5, 1, 1.5, 2, 2.5,) and (b) TEM image of Cs_2-TPA particles.

2.3. Proton conductivity (σ) and methanol permeability measurement

The membrane proton conductivities were measured using the four-point probe technique (in plane) which used four equally spaced probes in contact with the measured material. The CTS/Cs_2-PTA membranes were cut into 10 mm × 30 mm strips and placed across four platinum foils with equal spacing of 5 mm. AC impedance measurements were carried out between frequencies of 0.1 and 100 kHz. The membrane conductivity was measured at 100% RH in the temperature range of 303–353 K. The samples were held for 30 min for each measurement conditions.

Methanol permeability was determined by using a diffusion cell method at room temperature. Methanol solution (2 mol/L) and water were placed on two different compartments of the diffusion cell, separated by the membrane. Magnetic stirrers were used in each compartment to ensure uniformity. A Shimadzu GC-2014C with a FID detector and a Agilent HP-INNOWAX column (30 mm × 0.25 mm) was used for methanol analysis, and the peak areas were converted to methanol concentration by using a calibration curve. The methanol diffusion coefficient was obtained by analyzing the methanol flux with time and calculated as shown below:

$$C_B(t) = \frac{APC_A(t - t_0)}{V_B L} \quad (3)$$

where C_B and C_A are the methanol concentration of permeated and feed side through the membrane, respectively, A, L and V_B are the effective area of membrane, the thickness and the volume of permeated compartment, respectively. P is the methanol diffusion coefficient. The CTS/Cs_2-PTA membrane was immersed in Milli-Q water before methanol diffusion coefficient measurement.

3. Results and discussions

3.1. XRD, SEM and EDS analysis

It is known that the $H_3PW_{12}O_{40}$ and their corresponding cesium salts have crystal structure of cubic Pn3m symmetry. As shown in Fig. 1a, three characteristic diffraction peaks of typical Keggin structure can be found in XRD patterns for all Cs_x-PTA samples (Matachowski et al., 2011; Sasca et al., 2011; Xu et al., 2010). With the increasing amount of Cs content, the diffraction peaks at 26° became wider, indicating the decreased gain sizes and change from long-range order to short-range order. The results confirmed the formation of Cs_x-PTA single phase (Matachowski et al., 2011). TEM analysis shows the uniform distribution of Cs_x-TPA particles with average particle size of ~120 nm as shown in Fig. 1b.

Fig. 2 is the SEM images of the CTS and CTS/Cs_2-PTA composite membranes and the distribution of the Cs_x-PTA particles in the membranes. All the membranes show uniform and dense surface. The submicron particles of cesium phosphotungstate salt became increasingly visible with the increasing content of Cs_x-PTA in membrane (Fig. 2b–d). The cross-section of typical CTS/Cs_2-PTA-5 wt% shows a dense and homogeneous structure without obvious phase separation or structure defects (Fig. 2e), indicating the good phase compatibility between Cs_x-PTA and CTS. Since Cs_x-PTA contained special Keggin structure which mainly provides proton channel, its distribution not only affects the physical properties of the membrane but also the proton conductivity. In order to verify the distribution of Cs_x-PTA inside the membrane, the cross-section was analyzed by tungsten (W) mapping EDS. The result indicates that the element W (green spot) is homogeneously dispersed in the membrane (Fig. 2f). The uniformly distributed Cs_2-PTA is critical for the continuous proton conducting channel and high proton conductivity of the composite membranes.

3.2. FT-IR and X-ray diffractometry

The characteristic functional groups of Cs_2-PTA, CTS and CTS/Cs_2-PTA-5 wt% were investigated by FTIR and the results are shown in Fig. 3(a). The absorption peaks observed at 1029 cm^{-1} and 1153 cm^{-1} which is characteristic of the saccharide structure of CTS are observed in both CTS and CTS/Cs_2-PTA-5 wt% membranes. For cesium salt, four characteristic peaks of its Keggin anion were observed at 1079 cm^{-1} (P–O_a in central tetrahedral), 987 cm^{-1} (W=O_d terminal oxygen in the Keggin structure), 889 cm^{-1} (W–O_b–W) and 802 cm^{-1} (W–O_c–W). These characteristic vibration bands were also shown in the infrared spectra of CTS/Cs_2-PTA-5 wt% membrane.

The effect of Cs_2-PTA fillers on the crystalline structures of chitosan matrix was also studied by the XRD (Fig. 3b). In agreement with that reported in the literature (Wang et al., 2008), the pristine CTS membrane (curve a in Fig. 3b) exhibits three characteristic peaks at 2θ = 11.8°, 18.8°, 21.6° and some other diffraction

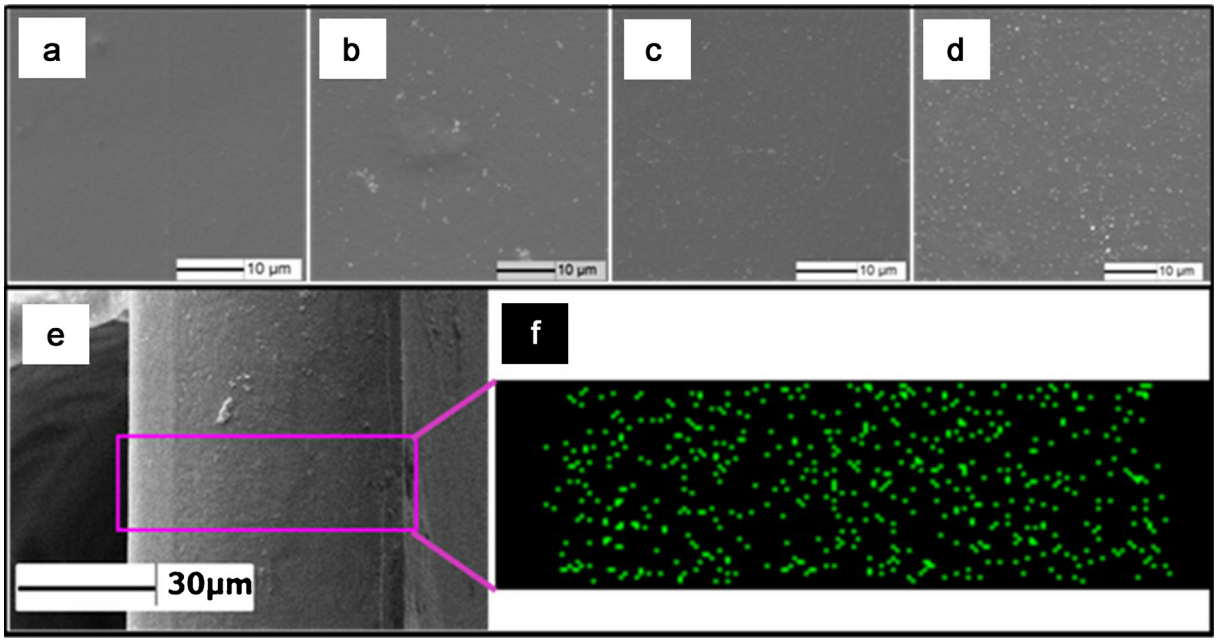

Fig. 2. The SEM morphology images and EDS of CTS/Cs_2-PTA composite membranes. The SEM images of the surface of CTS (a), CTS/Cs_2-PTA-1 wt% (b), CTS/Cs_2-PTA-5 wt% (c), CTS/Cs_2-PTA-10 wt% (d) membranes and the cross-section of CTS/Cs_2-PTA-5 wt% membrane (e). And the corresponding tungsten element (W) mapping EDS of CTS/Cs_2-PTA-5 wt% membrane is shown in (f).

peaks due to the semi-crystalline nature of chitosan. For the hybrid membranes, the incorporation of fillers interfered with the ordered packing of the chitosan chains by steric effects, thus destroying the crystalline domain of chitosan matrix. Accordingly, the peak intensity of the chitosan became weaker (curve b in Fig. 3b). In addition, the new peaks in XRD patterns of CTS/Cs_2-PTA-5 wt% membranes were attributed to the crystalline structure of Cs_2-PTA (Volkova et al., 2002).

3.3. The thermal stability and mechanical properties of CTS/Cs_2-PTA composite membranes

Fig. 4 is the TGA curves of CTS and CTS/Cs_2-PTA composite membranes. The CTS/Cs_2-PTA membranes maintain a good thermal stability, similar to that of the pure chitosan. The CTS-based membranes show three major weight loss stages around 40–120 °C, 220–320 °C, and 350–500 °C in the tested temperature range. In the first stage of 40–120 °C, the weight loss is ~10% and the lost is mainly due to the physically absorbed water (Cui et al., 2008). The thermal degradation of membranes took place at a maximum rate in the temperature range from 220 °C to 320 °C. More than 35% weight loss can be due to the cleavage of CTS chains and removal of bound water molecules from Cs_x-PTA. In the third stage, above 350 °C, the weight loss is assigned to structure collapse of Cs_x-PTA and the thermal decomposition of glucosamine residues present in CTS. So it can be concluded that the composite membrane is stable at desired operating temperatures (<100 °C) for DMFCs.

It is generally known that the water content has great influence on the proton conductivity as well as the stability of polymer electrolyte membrane. The existence of water molecular which was required for the proton transport also resulted in the dimensional change of the membranes. The results of measured water uptake

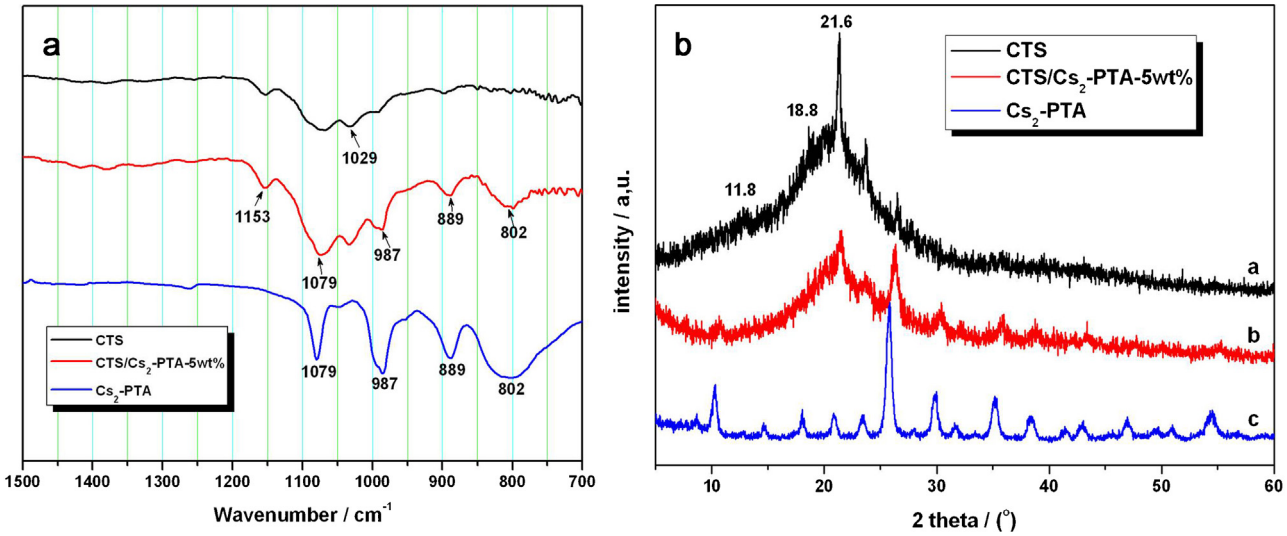

Fig. 3. The segment FT-IR spectra (a) and XRD patterns (b) of Cs_2-PTA powder, CTS and CTS/Cs_2-PTA-5 wt% membranes.

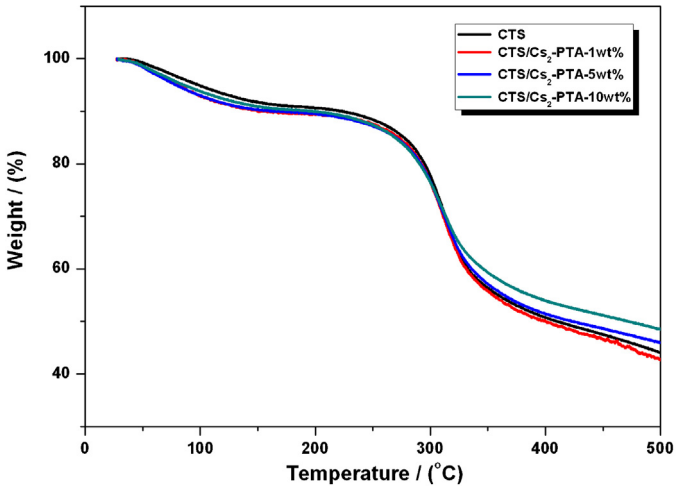

Fig. 4. TGA results of CTS/Cs_2-PTA membranes with different Cs_2-PTA doping content (0 wt%, 1 wt%, 5 wt%, 10 wt%).

and swelling ratio for the composite membranes were showed in Table S1 (see in supplementary data). For the purpose of comparison, data for Nafion 212 membrane is also included in the Table S1. The water uptake of CTS membrane is 60.1%, significantly higher than that of Nafion-212. The high hydrophilicity of CTS membrane is attributed to the active groups in chitosan molecular backbone. By blending with Cs_x-PTA, the water uptake and the swelling ratio of the membranes are further increased and the high Cs_2-PTA content in the composite membrane leads to a higher water uptake and higher swelling ratio. This phenomenon can be explained by the existence of heteropoly anions which could contain water molecule through weak hydrogen bond.

CTS membrane that prepared by traditional process presented strong elasticity and high moisture content under wet state, thus resulted in weak tensile strength (7.3 MPa, black line in Fig. 5). Meanwhile, the CTS membrane will lose most elasticity and turn into brittle material in the dehydration state. These mechanical behaviors suggested the CTS membrane by traditional process might be easily destroyed in the hot-pressing process of the membrane electrode assembly (MEA). Fig. 5 depicts mechanical properties of all the membranes studied here by determining the tensile strength. The data suggest that the tensile strength for the CTS/Cs_x-PTA composite membranes increases

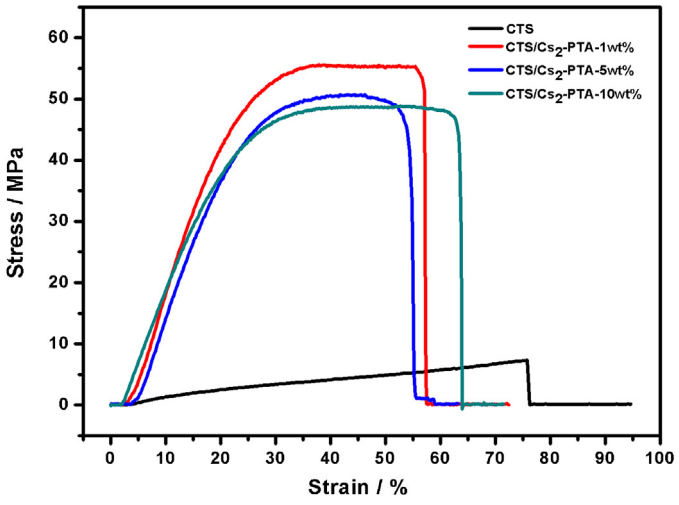

Fig. 5. The strain–stress curves of CTS/Cs_2-PTA-1 wt%, CTS/Cs2-PTA-5 wt%, CTS/Cs2-PTA-10 wt% and CTS membranes.

Table 1
The proton conductivity of CTS/Cs_x-PTA membranes with different Cs salt doping content at 25 °C ($\times 10^{-3}$ S cm^{-1}).

Value of x	Content of $Cs_xH_{3-x}PW_{12}O_{40}$		
	1 wt%	5 wt%	10 wt%
1	2.52	4.17	1.78
1.5	2.70	2.96	2.09
2	4.51	6.00	3.92
2.5	3.13	5.11	3.15

obviously (~50 MPa), which much higher than that of Nafion-212 (23.6 MPa). The reason may be that the introduction of Cs_x-PTA to CTS restricts the chain segmental mobility and increases the membrane strength. In addition, the Keggin structure of Cs_x-PTA cross-linked with the amino of CTS in a certain extent, which enhanced the mechanical properties of composite membranes. Thus, CTS/Cs_x-PTA composite membranes could completely achieve the requirements of fuel cell in the application of proton exchange membrane.

3.4. Proton conductivity (σ) of CTS/Cs_2-PTA composite membranes

For a polymer electrolyte membrane to be a good proton exchange membrane, it should contained fixed charged sites surrounded by water molecules, which facilitate the transport of protons (Amirinejad, Madaeni, & Navarra, 2011). Proton transport in CTS/Cs_x-PTA membrane is the result of a complex process dominated by the surface and chemical properties of both chitosan and Cs_x-PTA additive. Thus, the molecule structure, surface area and acid site density on Cs_x-PTA surface and water content of the membrane may have influence on conductivity of composite membranes (Matachowski et al., 2011; Okuhara, Watanabe, Nishimura, Inumaru, & Misono, 2000). We firstly investigated the effect of Cs content (x from 0.5 to 2.5) on proton conductivity of CTS/Cs_x-PTA membranes with 1 wt%, 5 wt% and 10 wt% Cs_x-PTA doping amount and the results are shown in Table 1. The conductivity was measured under 100% relative humidity at 25 °C. The measured conductivity is in the range of 2–6 $\times 10^{-3}$ S cm^{-1} and varies with both the Cs_x-PTA content in the composite membrane and the Cs content in PTA. Cs_x-PTA at $x = 2$ produced the highest proton conductivity for the CTS/Cs_x-PTA composite membranes prepared in this study, which was consistent with Shukla's result (Mohanapriya et al., 2009). Thus, in this study, Cs_2-PTA was used as standard filler in the composite membrane. The best results were obtained on CTS/Cs_2-PTA-5 wt% composite membrane, reaching 6 $\times 10^{-3}$ S cm^{-1}. Since chitosan itself has disordered structure, the results that CTS/Cs_2-PTA membranes displayed better performance might related to the excellent surface acidity of Cs_x-PTA at $x = 2$, numbers of sorption water and the surface area of particles as well as the interaction between the active groups of chitosan and Keggin structure (Okuhara et al., 2000; Yu, Guo, Xu, Yang, & Guo, 2008).

To evaluate the stability of Cs_x-PTA NPs in CTS, the sample was soaked in Milli-Q water, and the proton conductivity was measured as a function of time. Fig. S1 shows the conductivity stability of the Cs_2-PTA/CTS membrane. In cases where HPW molecules leaked from the Cs_x-PTA/CTS, the conductivity of composite membrane would decrease. However, the stability of proton conductivity indicated that Cs_x-PTA/CTS composite membrane was rather stable in a water system and that the Cs_x-PTA did not leach out, which also indicated that the interaction between the active groups of chitosan and Keggin structure of Cs_xPTA NPs.

Fig. 6 showed the proton conductivity of the CTS and CTS/Cs_2-PTA composite membranes under different temperature. The

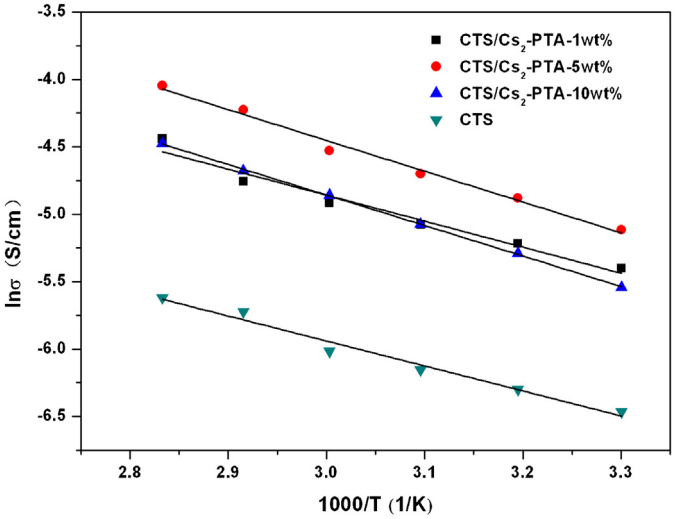

Fig. 6. Arrhenius plots of the proton conductivity of CTS membrane and CTS/Cs_2-PTA composite membranes.

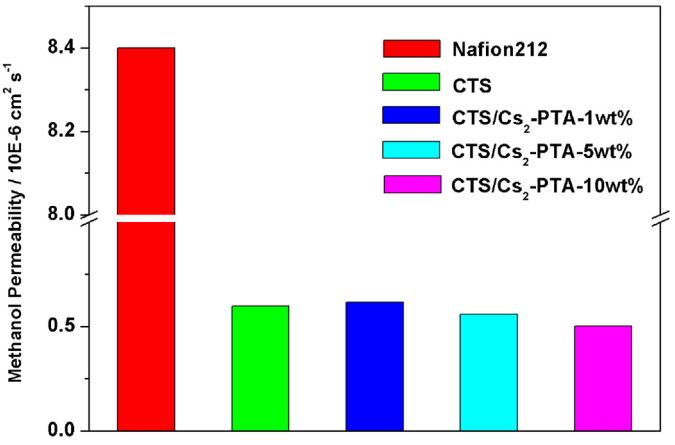

Fig. 7. The methanol permeability of Nafion-212 and CTS/Cs_2-PTA composite membranes with different Cs_2-PTA mixing ratios at 303 K.

conductivity for all the membranes increases with the increasing in temperature. The maximum proton conductivity observed for the CTS membrane is 3.63×10^{-3} S cm^{-1} at 353 K. The proton conductivity of the CTS/Cs_2-PTA composite membrane is 1.75×10^{-2} S cm^{-1} at 353 K, which is higher than that for the membrane without Cs_2-PTA. It is noteworthy that the CTS/Cs_2-PTA-5 wt% composite membrane exhibits higher proton conductivity than that of CTS/Cs_2-PTA-1 wt% and CTS/Cs_2-PTA-10 wt% membranes in the temperature range studied. This indicates that Cs_2-PTA nanoparticles within the CTS matrix act as proton carrier for the proton transfer through the composite membrane. The activation energy for proton transfer is 16.04, 18.97, 18.81 kJ/mol for CTS/Cs_2-PTA-1 wt%, CTS/Cs_2-PTA-5 wt% and CTS/Cs_2-PTA-10 wt%, respectively, close to 15.41 kJ/mol observed on pristine CTS membranes. The similarity in the activation energy for CTS and CTS/Cs_2-PTA composite membranes indicates that the proton transfer is most likely though the diffusion or vehicular pathway (Kreuer, Dippel, Meyer, & Maier, 1992). The vehicular mechanism for proton transfer is most likely due to the high water uptake of the membrane (see Table S1) as high water content facilitates proton transport through the membrane. In the case of CTS/Cs_2-PTA-1 wt% composite membrane, the number of Cs_2-PTA is low, leading to the low number of protons available within the membrane structure and thus relatively low proton conductivity. As the Cs_2-PTA filler content increases, the proton conductivity of the CTS/Cs_2-PTA composite membrane increases due to the increased number of proton carrier. However presence of excess Cs_2-PTA nanoparticles may inhibit the proton transfer probably due to the interface or boundary effect. This appears to explain the observation of the best proton conductivity on CTS/Cs_2-PTA composite membrane with 5 wt% Cs_2-PTA.

As indicated by Kozhevnikov, proton transport would most likely occur on the surface of the crystalline PTA (Kozhevnikov, 1998). Thus, it may be considered that Cs_x-TPA nanoparticles provide additional surface functional sites for proton transfer in CTS/Cs_x-TPA composite membranes. The schematic of the proton transfer mechanism through the CTS/Cs_x-PTA composite membranes was shown in Fig. S2. The proton transport can occur from the H_3O^+ as proton donor to the H_2O as acceptor on the Cs_x-TPA surface. Uniform distribution and optimum number of Cs_x-TPA nanoparticles within the composite membrane is critical for the continuous proton transfer pathway with minimum resistance, as shown above.

3.5. Methanol permeability of CTS/Cs_2-PTA and selectivity factors

Fig. 7 is the methanol permeability of Nafion-212, CTS and CTS/Cs_2-PTA composite membranes measured at room temperature. CTS and CTS/Cs_2-PTA composite membranes have much lower methanol permeability as compared to that of Nafion-212. For example, the methanol permeability of the CTS/Cs_2-PTA-5 wt% composite membrane is 5.6×10^{-7} cm^2 s^{-1} which is 90% lower than that of Nafion-212 membrane, demonstrating its excellent methanol crossover resistance. The introduction of Cs_2-PTA nanoparticles has no significant effect on the methanol permeability of chitosan membrane. Nevertheless, the methanol permeability slightly decreased with increased doping amount of Cs_2-PTA.

To achieve better cell performance of DMFC, it is important to obtain higher proton conductivity and lower methanol permeability simultaneously. The ratio of the proton conductivity to the methanol permeability can be defined as the membrane selectivity factor (φ) and may be used as an indicator of the suitability of a given membrane for DMFC applications (Xu et al., 2010). As shown in Table S2, the CTS/Cs_2-PTA with 5 wt% Cs_2-PTA exhibits the highest selectivity factor. This indicates that CTS/Cs_2-PTA-5 wt% composite membrane is most suitable for the PEM application of direct methanol fuel cells.

4. Conclusion

A novel CTS/Cs_x-PTA composite membrane was successfully prepared and characterized for potential application as proton exchange membranes of DMFCs. The proton conductivity of the composite membranes is a function of both the Cs_x-PTA content in the composite membrane and the Cs substitution in PTA. Cs_x-PTA at $x = 2$ produced the highest proton conductivity for the CTS/Cs_x-PTA composite membranes with Cs_2-PTA content of 5 wt%. The proton conductivity of CTS/Cs_2-PTA membrane reached 1.75×10^{-2} S cm^{-1} at 353 K. The FT-IR, TG, EDS elemental mapping examination indicated that the Cs_2-PTA nanoparticles were uniformly distributed in the chitosan matrix. In addition, the mechanical properties of the composite membrane are much better than that of the conventional Nafion membrane. The methanol permeability of CTS/Cs_2-PTA membrane is about 5.6×10^{-7} cm^2 s^{-1}, 90% lower than that of Nafion-212 membrane. The highest selectivity factor was obtained on CTS/Cs_2-PTA-5 wt% composite membrane, indicating its promising potential as alternative PEMs of DMFCs.

Acknowledgements

This work was financially supported by grants from the National Natural Science Foundation of China (Nos. 21003007, U1137602, 21073010), National High Technology Research and Development Program of China (863 program, 2013AA031902), National Basic Research Program (973 Program) (No. 2011CB935700), National Science Foundation of Beijing, China (No. 2132051), and Program for New Century Excellent Talents in University. The authors are grateful to Prof. San Ping Jiang (Fuels and Energy Technology Institute & Department of Chemical Engineering, Curtin University) for useful discussions and manuscript proof reading.

Appendix A. Supplementary data

Supplementary data associated with this article can be found, in the online version, at http://dx.doi.org/10.1016/j.carbpol.2013.06.017.

References

Amirinejad, M., Madaeni, S. S., & Navarra, M. A. (2011). Preparation and characterization of phosphotungstic acid-derived salt/Nafion nanocomposite membranes for proton exchange membrane fuel cells. *Journal of Power Sources*, *196*, 988–998.

Amirinejad, M., Madaeni, S. S., & Rafiee, E. (2011). Cesium hydrogen salt of heteropolyacids/Nafion nanocomposite membranes for proton exchange membrane fuel cells. *Journal of Membrane Science*, *377*, 89–98.

Amirinejad, M., Madaeni, S. S., Navarra, M. A., Rafiee, E., & Scrosati, B. (2010). Solvent-free nanocomposite proton-conducting membranes composed of cesium salt of phosphotungstic acid doped PVDF-CTFE/PEO blend. *Ionics*, *16*, 681–687.

Chai, Z., Wang, C., Zhang, H., Doherty, C. M., Ladewig, B. P., Hill, A. J., et al. (2010). Nafion-carbon nanocomposite membranes prepared using hydrothermal carbonization for proton-exchange-membrane fuel cells. *Advanced Functional Materials*, *20*(24), 4394–4399.

Chávez, E. L., Oviedo-Roa, R., Contreras-Pérez, G., Martínez-Magadán, J. M., & Castillo-Alvarado, F. L. (2010). Theoretical studies of ionic conductivity of crosslinked chitosan membranes. *International Journal of Hydrogen Energy*, *35*(21), 12141–12146.

Cui, Z., Xiang, Y., Si, J. J., Yang, M., Zhang, Q., & Zhang, T. (2008). Ionic interactions between sulfuric acid and chitosan membranes. *Carbohydrate Polymers*, *73*(1), 111–116.

Cui, Z. M., Xing, W., Liu, C. P., Liao, J. H., & Zhang, H. (2009). Chitosan/heteropolyacid composite membranes for direct methanol fuel cell. *Journal of Power Sources*, *188*(1), 24–29.

Doğan, H., Inan, T. Y., Unveren, E., & Kaya, M. (2010). Effect of cesium salt of tungstophosphoric acid (Cs-TPA) on the properties of sulfonated polyether ether ketone (SPEEK) composite membranes for fuel cell applications. *International Journal of Hydrogen Energy*, *35*(15), 7784–7795.

Du, C. Y., Zhao, T. S., & Yang, W. W. (2007). Effect of methanol crossover on the cathode behavior of a DMFC: A half-cell investigation. *Electrochimica Acta*, *52*(16), 5266–5271.

Eccarius, S., Garcia, B. L., Hebling, C., & Weidner, J. W. (2008). Experimental validation of a methanol crossover model in DMFC applications. *Journal of Power Sources*, *179*(2), 723–733.

Ghazali, M., Nawawi, M., & Huang, R. Y. M. (1997). Pervaporation dehydration of isopropanol with chitosan membranes. *Journal of Membrane Science*, *124*(1), 53–62.

Jiang, Z. Y., Zheng, X. H., Wu, H., Wang, J. T., & Wang, Y. B. (2008). Proton conducting CS/P(AA-AMPS)membrane with reduced methanol permeability for DMFCs. *Journal of Power Sources*, *180*(1), 143–153.

Khiar, A. S. A., Puteh, R., & Arof, A. K. (2006). Conductivity studies of a chitosan-based polymer electrolyte. *Physica B: Condensed Matter*, *373*(1), 23–27.

Kozhevnikov, I. V. (1998). Catalysis by heteropoly acids and multicomponent polyoxometalates in liquid-phase reactions. *Chemical Reviews*, *98*(1), 171–198.

Kreuer, K.-D., Dippel, T., Meyer, W., & Maier, J. (1992). Nafion® membranes: Molecular diffusion, proton conductivity and proton conduction mechanism. *MRS Online Proceedings Library*, *293*

Li, L., Xu, L., & Wang, Y. (2003). Novel proton conducting composite membranes for direct methanol fuel cell. *Materials Letters*, *57*(8), 1406–1410.

Li, M.-Q., Shao, Z.-G., & Scott, K. (2008). A high conductivity $Cs_{2.5}H_{0.5}PMo_{12}O_{40}$/polybenzimidazole (PBI)/H_3PO_4 composite membrane for proton-exchange membrane fuel cells OPE-rating at high temperature. *Journal of Power Sources*, *183*(1), 69–75.

Li, M. Q., Shao, Z. G., & Zhang, H. M. E. A. (2006). Self-humidifying $Cs_{2.5}H_{0.5}PW_{12}O_{40}$/Nafion/PTFE composite membrane for proton exchange membrane fuel cells. *Electrochemical and Solid-State Letters*, *9*(2), A92–A95.

Ma, J., & Sahai, Y. (2013). Chitosan biopolymer for fuel cell applications. *Carbohydrate Polymers*, *92*(2), 955–975.

Ma, J., Sahai, Y., & Buchheit, R. G. (2012). Evaluation of multivalent phosphate cross-linked chitosan biopolymer membrane for direct borohydride fuel cells. *Journal of Power Sources*, *202*, 18–27.

Ma, Z. N., Hua, W. M., Ren, Y., He, H. Y., & Gao, Z. (2003). N-Butane isomerization over Cs-salts of $H_3PW_{12}O_{40}$: A mechanistic study by 1C MAS NMR. *Applied Catalysis A: General*, *256*(1–2), 243–250.

Majid, S. R., & Arof, A. K. (2005). Proton-conducting polymer electrolyte films based on chitosan acetate complexed with NH_4NO_3 salt. *Physica B: Condensed Matter*, *355*(1–4), 78–82.

Matachowski, L., Drelinkiewicz, A., Lalik, E., Mucha, D., Gil, B., Brożek-Mucha, Z., et al. (2011). The influence of reagent used for the precipitation of $Cs_2HPW_{12}O_{40}$ salt on its textural and catalytic properties. *Microporous and Mesoporous Materials*, *144*(1–3), 46–56.

Matsuda, A., Kikuchi, T., Katagiri, K., Daiko, Y., Muto, H., & Sakai, M. (2007). Mechanochemical synthesis of proton conductive cesium hydrogen salts of 12-tungstophosphoric acid and their composites. *Solid State Ionics*, *178*(7–10), 723–727.

Mochizuki, A., Amiya, S., Sato, Y., Ogawara, H., & Yamashita, S. (1989). Pervaporation separation of water/ethanol mixtures through polysaccharide membranes. III. The permselectivity of the neutralized chitosan membrane and the relationships between its permselectivity and solid state structure. *Journal of Applied Polymer Science*, *37*(12), 3385–3398.

Mohanapriya, S., Bhat, S. D., Sahu, A. K., Pitchumani, S., Sridhar, P., & Shukla, A. K. (2009). A new mixed-matrix membrane for DMFCs. *Energy & Environmental Science*, *2*(11), 1210–1216.

Muzzarelli, R. A. A. (2011). Potential of chitin/chitosan-bearing materials for uranium recovery: An interdisciplinary review. *Carbohydrate Polymers*, *84*(1), 54–63.

Odeh, A. O., Osifo, P., & Noemagus, H. (2013). Chitosan: A low cost material for the production of membrane for use in PEMFC—a review. *Energy Sources, Part A: Recovery, Utilization, and Environmental Effects*, *35*(2), 152–163.

Oh, S.-Y., Yoshida, T., Kawamura, G., Muto, H., Sakai, M., & Matsuda, A. (2010). Inorganic–organic composite electrolytes consisting of polybenzimidazole and Cs-substituted heteropoly acids and their application for medium temperature fuel cells. *Journal of Materials Chemistry*, *20*(30), 6359–6366.

Okuhara, T., Watanabe, H., Nishimura, T., Inumaru, K., & Misono, M. (2000). Microstructure of cesium hydrogen salts of 12-tungstophosphoric acid relevant to novel acid catalysis. *Chemistry of Materials*, *12*(8), 2230–2238.

Osifo, P. O., & Masala, A. (2012). The influence of chitosan membrane properties for direct methanol fuel cell applications. *Journal of Fuel Cell Science and Technology*, *9*(1), 011003-1–011003-9.

Qi, Z. G., & Kaufman, A. (2002). Open circuit voltage and methanol crossover in DMFCs. *Journal of Power Sources*, *110*(1), 177–185.

Sancho, T., Soler, J., & Pina, M. P. (2007). Conductivity in zeolite–polymer composite membranes for PEMFCs. *Journal of Power Sources*, *169*(1), 92–97.

Sasca, V., Verdeş, O., Avram, L., Popa, A., Barvinschi, P., & Mracec, M. (2011). Non-isothermal kinetics study of the constitutional water loss from 12-tungstophosphoric acid and some of its acidic cesium salts. *Revue Roumaine de Chimie*, *56*(5), 501–516.

Seo, J. A., Koh, J. H., Roh, D. K., & Kim, J. H. (2009). Preparation and characterization of crosslinked proton conducting membranes based on chitosan and PSSA–MA copolymer. *Solid State Ionics*, *180*(14–16), 998–1002.

Smitha, B., Devi, D. A., & Sridhar, S. (2008). Proton-conducting composite membranes of chitosan and sulfonated polysulfone for fuel cell application. *International Journal of Hydrogen Energy*, *33*(15), 4138–4146.

Smitha, B., Sridhar, S., & Khan, A. A. (2005). Synthesis and characterization of poly(vinyl alcohol)-based membranes for direct methanol fuel cell. *Journal of Applied Polymer Science*, *95*(5), 1154–1163.

Suzuki, K., Saimoto, H., & Shigemasa, Y. (1999). Electric resistance of chitosan derivatives. *Carbohydrate Polymers*, *39*(2), 145–150.

Tang, H., Wang, X., Pan, M., & Wang, F. (2007). Fabrication and characterization of improved PFSA/ePTFE composite polymer electrolyte membranes. *Journal of Membrane Science*, *306*(1–2), 298–306.

Tang, H. L., Pan, M., Jiang, S. P., & Yuan, R. Z. (2005). Modification of Nafion™ membrane to reduce methanol crossover via self-assembled Pd nanoparticles. *Materials Letters*, *59*(28), 3766–3770.

Tang, H. L., Pan, M., & Wang, F. (2008). A mechanical durability comparison of various perfluocarbon proton exchange membranes. *Journal of Applied Polymer Science*, *109*(4), 2671–2678.

Tang, H. L., Wang, S. L., Pan, M., Jiang, S. P., & Ruan, Y. Z. (2007). Performance of direct methanol fuel cells prepared by hot-pressed MEA and catalyst-coated membrane (CCM). *Electrochimica Acta*, *52*(11), 3714–3718.

Tricoli, V., Carretta, N., & Bartolozzi, M. (2000). Comparative investigation of proton and methanol transport in fluorinated ionomeric membranes. *Journal of Electrochemical Society*, *147*(4), 1286–1290.

Volkova, G. G., Plyasova, L. M., Salanov, A. N., Kustova, G. N., Yurieva, T. M., & Likholobov, V. A. (2002). Heterogeneous catalysts for halide-free carbonylation of dimethyl ether. *Catalysis Letters*, *80*(3–4), 175–179.

Wan, Y., Creber, K. A. M., Peppley, B., & Bui, V. T. (2003a). Ionic conductivity of chitosan membranes. *Polymer*, *44*(4), 1057–1065.

Wan, Y., Creber, K. A. M., Peppley, B., & Bui, V. T. (2003b). Synthesis, characterization and ionic conductive properties of phosphorylated chitosan membranes. *Macromolecular Chemistry and Physics*, *204*(5–6), 850–858.

Wang, J. T., Zheng, X. H., Wu, H., Zheng, B., Jiang, Z. Y., Hao, X. P., et al. (2008). Effect of zeolites on chitosan/zeolite hybrid membranes for direct methanol fuel cell. *Journal of Power Sources*, *178*(1), 9–19.

Wu, H., Hou, W., Wang, J., Xiao, L., & Jiang, Z. (2010). Preparation and properties of hybrid direct methanol fuel cell membranes by embedding organophosphorylated titania submicrospheres into a chitosan polymer matrix. *Journal of Power Sources*, *195*(13), 4104–4113.

Xu, D., Zhang, G., Zhang, N., Li, H., Zhang, Y., Shao, K., et al. (2010). Surface modification of heteropoly acid/SPEEK membranes by polypyrrole with a sandwich structure for direct methanol fuel cells. *Journal of Materials Chemistry*, *20*(41), 9239–9245.

Yamada, M., & Honma, I. (2005). Anhydrous proton conductive membrane consisting of chitosan. *Electrochimica Acta*, *50*, 2837–2841.

Yang, J., Janik, M. J., Ma, D., Zheng, A., Zhang, M., Neurock, M., et al. (2005). Location, acid strength, and mobility of the acidic protons in Keggin 12-H3PW12O40: A combined solid-state NMR spectroscopy and DFT quantum chemical calculation study. *Journal of the American Chemical Society*, *127*(51), 18274–18280.

Yang, J. H., & Bae, Y. C. (2008). Methanol crossover effect for direct methanol fuel cells: Applicability of methanol activity in polymer electrolyte membrane. *Journal of The Electrochemical Society*, *155*(2), B194–B199.

Yang, M., Lu, S., Lu, J., Jiang, S. P., & Xiang, Y. (2010). Layer-by-layer self-assembly of PDDA/PWA-Nafion composite membranes for direct methanol fuel cells. *Chemical Communications*, *46*(9), 1434–1436.

Yu, X. D., Guo, Y. N., Xu, L. L., Yang, X., & Guo, Y. H. (2008). A novel preparation of mesoporous $Cs_xH_{3-x}PW_{12}O_{40}/TiO_2$ nanocomposites with enhanced photocatalytic activity. *Colloids and Surfaces A: Physicochemical and Engineering Aspects*, *316*(1–3), 110–118.

Zhang, Y., Zhang, H. M., & Bi, C. (2008). An inorganic/organic self-humidifying composite membranes for proton exchange membrane fuel cell application. *Electrochimica Acta*, *53*, 4096–4103.